for the Cu^+/Cu^{2+} pair than previously thought.

We have not attempted any calculation of the rate constant for electron transfer. This would require detailed information of the energy surfaces and is not feasible within the EH model used here. Due to the complicated nature of biological structures it is doubtful whether any quantum chemical method in current use could contribute to the solution of this problem.

Acknowledgment. I am grateful to A. Bárány, B. Roos, and T. Andersson for helpful discussions and to M. D. Newton for sending a manuscript (ref 19) prior to publication. This work was supported by NFR, the Swedish Natural Science Research Council. I am finally grateful to the members of the Centre for Chemical Physics, University of Western Ontario, London, Canada, where this work was started, for support and hospitality.

Molecular and Electronic Structures of Two Quadruply Bonded Ditungsten Compounds and a Dimolybdenum Homologue

F. Albert Cotton,*[1a] Michael W. Extine,[1b] Timothy R. Felthouse,[1a] Brian W. S. Kolthammer,[1a] and Dennis G. Lay[1a]

Contribution from the Department of Chemistry, Texas A&M University, College Station, Texas 77843. *Received January 2, 1981*

Abstract: The structures of the isomorphous compounds $W_2Cl_4(PMe_3)_4$ (**1a**) and $Mo_2Cl_4(PMe_3)_4$ (**1b**) and also that of $W_2Cl_4(Me_2PCH_2CH_2PMe_2)_2$ (**2**) are reported and discussed. Compounds **1a** and **1b** crystallize in space group $C2/c$ with the following unit cell parameters (each given for **1a** and **1b** in that order): a = 18.296 (3) Å, 18.369 (2) Å; b = 9.192 (2) Å, 9.172 (2) Å; c = 17.274 (2) Å, 17.331 (4) Å; β = 115.34 (1)°, 115.33 (1)°; V = 2626 (2) Å^3, 2639 (2) Å^3. With Z = 4 each molecule lies on a special position with the M–M bond coincident with a crystallographic twofold axis. The structures have been refined to R_1 = 0.027, 0.018 and R_2 = 0.038, 0.027 with inclusion of all hydrogen atoms. The sets of chlorine and phosphine ligands are staggered within themselves while the overall ligand arrangement about the dimetal unit defines an eclipsed conformation. The approximate symmetry is D_{2d}. The metal–metal bond lengths are 2.262 (1) and 2.130 (1) Å for **1a** and **1b**, respectively. Crystals of **2** belong to the space group $P2_1/n$ with a cell of dimensions a = 9.150 (2) Å, b = 12.029 (1) Å, c = 14.245 (2) Å, and β = 105.88 (2)°. The structure has been refined to R_1 = 0.029 and R_2 = 0.038. Two tungsten dimers and a toluene molecule reside on crystallographic centers of inversion within the unit cell. One dmpe ligand is chelated to each metal atom, and to satisfy the center of inversion, the entire arrangement of ligands then corresponds approximately to C_{2h} symmetry. The W–W distance is 2.287 (1) Å. The UV–visible spectra of **1a** and **1b** are reported, and the variations in M–Cl and M–P distances as a function of cis and trans stereochemistry as well as the change from Mo to W are discussed.

The preparation [2] and structural characterization[3] of quadruply bonded ditungsten compounds of the type $W_2X_4(PR_3)_4$, where the four PR_3 ligands may also be replaced by two diphosphines, has recently been reported in preliminary form. A series of papers describing this work in detail, of which this is the first, will be appearing in the near future.

In this paper we report the structures of the three compounds $W_2Cl_4(PMe_3)_4$ (**1a**), its molybdenum analogue $Mo_2Cl_4(PMe_3)_4$ (**1b**), and $W_2Cl_4(dmpe)_2$ (**2**), where dmpe is a code for $Me_2PCH_2CH_2PMe_2$. The particular points of interest, upon which the decision to cover these three compounds together in one paper was based, are the following: (1) the comparison of **1a** and **1b** provides new insight into the similarities, and differences, between molybdenum and tungsten in their capacity for the formation of multiple M–M bonds; (2) the comparison of **1a** and **2** affords the first opportunity to evaluate the effect of changing the geometric arrangement of ligands on each metal atom from trans to cis while making, as nearly as possible, no change in the nature of the ligands themselves. Compound **2** is also interesting intrinsically because it is the first example of a chelating, rather than bridging, diphosphine ligand in dinuclear, multiply bonded M–M chemistry.

Experimental Section

All chemicals used were of reagent grade or of comparable purity. All reagents were purchased from commercial suppliers. All manipulations were carried out under anhydrous anaerobic conditions unless otherwise specified. Tungsten(IV) chloride was prepared by the sodium amalgam reduction of WCl_6 in tetrahydrofuran.

Mass spectral measurements were performed at 10 eV on an AEI MS902 mass spectrometer.[4] These spectra were obtained by the direct probe insertion method with an ionization chamber temperature of 190 °C. A Cary 17 spectrophotometer was employed to obtain solution UV–visible spectra of **1a** and **1b**.

Preparation of the $M_2Cl_4(PMe_3)_4$ Complexes. The tungsten compound **1a** was prepared according to the literature method[2] by the alkali metal reduction of WCl_4 in the presence of 2 equiv of trimethylphosphine. The green product was purified by filtering a toluene solution of $W_2Cl_4(PMe_3)_4$ through a 3 × 6 cm column of Florisil. The filtrate was concentrated in vacuo and cooled to −10 °C to induce crystallization of complex **1a**.

The molybdenum analogue was prepared by stirring a suspension of $K_4Mo_2Cl_8$[5] in methanol at room temperature in the presence of a twofold excess of trimethylphosphine. After 70 h, the red starting material had been replaced by a dark blue solid. This precipitate was collected, washed with water, and dried under vacuum. Compound **1b** was further purified by dissolution in a minimum amount of toluene followed by filtration of the resulting solution through a 3 × 10 cm column of Florisil and removal of the solvent under reduced pressure.

X-ray Diffraction Studies. Single crystals of compound **1b** suitable for crystallographic study were obtained by slow cooling of a toluene solution from room temperature to −10 °C. Crystals of complexes **1a** and **2** were obtained from Professor R. R. Schrock. Crystals were examined by using the automatic search routine on an Enraf-Nonius CAD-4 dif-

(1) (a) Texas A&M University. (b) Molecular Structure Corporation.
(2) Sharp, P. R.; Schrock, R. R. *J. Am. Chem. Soc.* **1980**, *102*, 1430.
(3) Cotton, F. A.; Felthouse, T. R.; Lay, D. G. *J. Am. Chem. Soc.* **1980**, *102*, 1431.
(4) Mass Spectral measurements were performed by Dr. G. Eigendorf of the University of British Columbia.
(5) Brencic, J. V.; Cotton, F. A. *Inorg. Chem.* **1969**, *8*, 7.

0002-7863/81/1503-4040$01.25/0 © 1981 American Chemical Society

Table I. Crystallographic Data and Enraf-Nonius CAD-4 Data Collection Procedures

	1a	1b	2
formula	$W_2Cl_4P_4C_{12}H_{36}$	$Mo_2Cl_4P_4C_{12}H_{36}$	$W_2Cl_4P_4C_{19}H_{40}$
M_r	813.83	638.01	901.94
space group	$C2/c$	$C2/c$	$P2_1/n$
a, Å	18.296 (3)	18.369 (2)	9.150 (2)
b, Å	9.192 (2)	9.172 (2)	12.029 (1)
c, Å	17.274 (2)	17.331 (4)	14.245 (2)
β, deg	115.34 (1)	115.33 (1)	105.88 (2)
V, Å^3	2626 (2)	2639 (2)	1508.1 (9)
Z	4	4	2
ρ(calcd), g/cm^3	2.06	1.61	1.99
cryst size, mm	0.1 × 0.1 × 0.2	0.2 × 0.2 × 0.3	0.2 × 0.2 × 0.3
μ(Mo Kα), cm^{-1}	99.153	15.673	86.431
radiation	graphite-monochromated Mo Kα ($\lambda_{\bar{\alpha}}$ = 0.71073 Å)		
scan type	ω–2θ	ω–2θ	ω–2θ
scan width ($\Delta\omega$), deg	0.70 + 0.35 tan θ	0.60 + 0.35 tan θ	0.70 + 0.35 tan θ
aperature width, mm	1.5 + tan θ	1.5 + tan θ	1.5 + tan θ
crystal-counter dist, mm	173	173	173
prescan rejection limit	2.0 (0.5σ)	2.0 (0.5σ)	2.0 (0.5σ)
prescan acceptance limit	0.05 (20σ)	0.02 (50σ)	0.05 (20σ)
max scan speed, deg/min	20.12	20.12	20.12
max counting time, s	30	30	30
collectn range	$+h,+k,\pm l$, $4° \leq 2\theta \leq 50°$		
no. of data collected	2467	2475	2957
no. of data with $I > 3\sigma(I)$	1741	1957	2082
p	0.05	0.05	0.05
X-ray exposure time, h	14	18	18
no. of intensity stds	3	3	3
time between measurements, s	3600	3600	3600
cryst decomp	negligible	negligible	negligible
no. of variables	101	173	183
R_1	0.027	0.018	0.029
R_2	0.038	0.027	0.038
esd	1.073	0.886	1.078
g	1.89 × 10^{-7}	5.91 × 10^{-7}	
largest parameter shift[a]	0.15	0.05	0.47
largest peak,[b] e Å^{-3}	0.71	0.15	0.34

[a] Final refinement cycle. [b] Largest peak in the final difference Fourier map.

fractometer, and ω scans of several strong reflections indicated in each case that the crystals were of satisfactory quality. A least-squares analysis of the setting angles of 25 reflections ($26 \leq 2\theta \leq 32°$), automatically located and centered, provided accurate unit cell parameters (Table I). The general procedures for data collection were as previously described,[6] and the CAD-4 parameters employed are summarized in Table I. All data sets were corrected for Lorentz and polarization effects, and, in addition, an absorption correction was applied to **1a** and **2**. These latter corrections were made by using an empirical method based on ψ scans (ψ = 0–360° every 10°) for χ values near 90°. For both, eight sets of ψ scans were used with maximum minimum and average relative transmission factors for **1a** of 1.00, 0.47, and 0.79 and for **2** of 1.00, 0.57, and 0.81, respectively.

The heavy-atom positions of **1a** were obtained from a three-dimensional Patterson function. Full-matrix least-squares refinement followed by a Fourier synthesis revealed the positions of all other nonhydrogen atoms. The structure was refined further by three cycles of least squares using anisotropic thermal parameters. A further Fourier synthesis revealed the positions of some of the hydrogen atoms. However, these atoms were not well behaved upon attempted refinement. Therefore, all hydrogen atom positions were calculated by assuming a staggered configuration and C–H distance of 0.95 Å. These atoms were assigned isotropic B values of $(1 + B_{iso})$, where B_{iso} is the converged isotropic equivalent of the C atom to which they were bonded. Least-squares refinement led to convergence with the final discrepancy indices given by $R_1 = \sum||F_o| - |F_c||/\sum|F_o|$ and $R_2 = [\sum w(|F_o| - |F_c|)^2/\sum w|F_o|^2]^{1/2}$ and listed in Table I.

The molybdenum complex, **1b**, was found to be isomorphous to **1a**, and its structure was refined as follows. The positional parameters for all nonhydrogen atoms obtained for **1a** were refined by full-matrix least squares using anisotropic thermal parameters. A Fourier synthesis revealed the positions of all hydrogens, and these were refined along with isotropic B values. The structure was refined to convergence with the final R_1 and R_2 values listed in Table I.

The heavy-atom positions of **2** were obtained from a three-dimensional Patterson function. A difference Fourier map contained peaks due to all nonhydrogen atoms following least-squares refinement of the tungsten atom positions. A full-matrix least-squares refinement including anisotropic thermal parameters was carried out. A further Fourier synthesis produced positional parameters for 16 of the 22 hydrogen atoms. The remaining six hydrogen positions were calculated (vide supra). All hydrogen atoms were assigned isotropic B values of 7.0 Å^2 and included in the refinement. The final discrepancy factors following convergence are listed in Table I.

A list of structure factors for each compound is available as supplementary material. Tables II, III, and IV contain positional and thermal parameters for compounds **1a**, **1b**, and **2**, respectively.

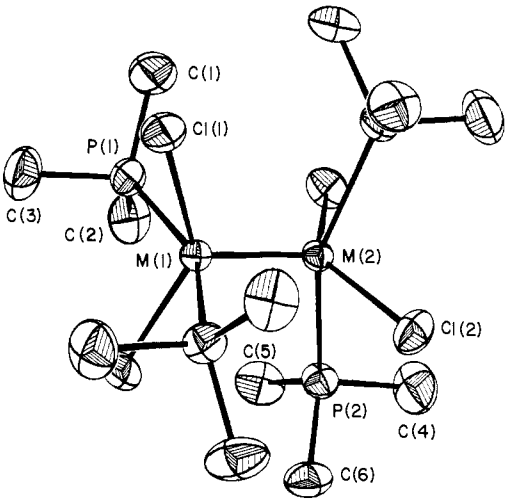

Figure 1. The molecular structure of the $M_2Cl_4(PMe_3)_4$ compounds **1a** and **1b**. Each atom is represented by its ellipsoid of thermal vibration scaled to enclose 40% of its electron density.

Results

Structures. Compounds **1a** and **1b** are crystallographically isomorphous, and the molecules are very closely similar. The molecular structure is shown in Figure 1, where the atom-labeling scheme is defined for **1a** and **1b** and the crystal packing may be seen in Figure 2. Table V gives the interatomic distances and bond angles for both compounds. A table of the C–H bond lengths and angles involving the hydrogen atoms (Table VA) is available as supplementary material. These distances and angles were all within the usual ranges for determinations of this type but were, as expected not very precise, with esd's on C–H distances running

(6) Bino, A.; Cotton, F. A.; Fanwick, P. E. *Inorg. Chem.* **1979**, *18*, 3558.
(7) Chisholm, M. H.; Cotton, F. A.; Extine, M. W.; Murillo, C. A. *Inorg. Chem.* **1978**, *17*, 2338 and references cited therein.

Table II. Positional and Thermal Parameters and Their Estimated Standard Deviations for $W_2Cl_4(PMe_3)_4$ (1a)[a,b]

atom	x	y	z	B(1,1)	B(2,2)	B(3,3)	B(1,2)	B(1,3)	B(2,3)
W(1)	0.0000 (0)	0.34157 (5)	0.2500 (0)	2.04 (1)	2.20 (2)	2.14 (1)	0	0.882 (8)	0
W(2)	0.0000 (0)	0.09553 (4)	0.2500 (0)	2.13 (1)	2.15 (2)	1.97 (1)	0	0.809 (9)	0
Cl(1)	−0.1034 (1)	0.4381 (2)	0.1208 (1)	3.52 (7)	3.45 (8)	3.34 (7)	0.69 (7)	0.57 (5)	0.73 (7)
Cl(2)	−0.0854 (1)	0.0001 (2)	0.3106 (1)	3.92 (6)	3.82 (9)	3.86 (6)	−0.96 (7)	2.22 (4)	0.07 (6)
P(1)	0.0952 (1)	0.3945 (2)	0.1836 (1)	3.10 (6)	3.16 (9)	3.54 (6)	−0.08 (6)	1.85 (5)	0.63 (6)
P(2)	−0.1151 (1)	0.0430 (2)	0.1077 (1)	3.13 (7)	3.12 (8)	2.35 (6)	−0.11 (7)	0.71 (5)	−0.26 (7)
C(1)	0.2007 (5)	0.340 (1)	0.2400 (6)	2.7 (3)	8.2 (6)	7.1 (4)	0.9 (4)	2.6 (2)	2.6 (4)
C(2)	0.0689 (5)	0.337 (1)	0.0747 (5)	7.1 (4)	4.7 (5)	4.4 (3)	−1.5 (4)	3.7 (2)	−0.2 (3)
C(3)	0.1018 (5)	0.589 (1)	0.1762 (6)	5.4 (4)	3.8 (5)	6.4 (4)	−0.6 (3)	3.1 (3)	0.4 (3)
C(4)	−0.1269 (6)	−0.153 (1)	0.0952 (6)	6.6 (5)	5.5 (5)	5.2 (4)	−1.1 (5)	1.2 (4)	−1.4 (4)
C(5)	−0.2154 (4)	0.097 (1)	0.0905 (5)	2.1 (3)	5.5 (5)	3.9 (3)	−0.2 (3)	0.4 (2)	0.3 (3)
C(6)	−0.1096 (5)	0.097 (1)	0.0093 (5)	5.0 (4)	6.6 (6)	2.7 (3)	0.2 (4)	1.6 (2)	−0.4 (3)

atom	x	y	z	B, Å²	atom	x	y	z	B, Å²
H(11)	0.2291 (0)	0.3666 (0)	0.2073 (0)	6.5300 (0)	H(41)	−0.1703 (0)	−0.1744 (0)	0.0414 (0)	6.7900 (0)
H(12)	0.2244 (0)	0.3864 (0)	0.2942 (0)	6.5300 (0)	H(42)	−0.0784 (0)	−0.1942 (0)	0.0977 (0)	6.7900 (0)
H(13)	0.2036 (0)	0.2371 (0)	0.2479 (0)	6.5300 (0)	H(43)	−0.1381 (0)	−0.1915 (0)	0.1399 (0)	6.7900 (0)
H(21)	0.1107 (0)	0.3649 (0)	0.0588 (0)	5.7800 (0)	H(51)	−0.2526 (0)	0.0700 (0)	0.0341 (0)	4.7400 (0)
H(22)	0.0626 (0)	0.2345 (0)	0.0708 (0)	5.7800 (0)	H(52)	−0.2296 (0)	0.0489 (0)	0.1309 (0)	4.7400 (0)
H(23)	0.0196 (0)	0.3822 (0)	0.0372 (0)	5.7800 (0)	H(53)	−0.2170 (0)	0.1989 (0)	0.0972 (0)	4.7400 (0)
H(31)	0.1376 (0)	0.6114 (0)	0.1511 (0)	6.0700 (0)	H(61)	−0.1580 (0)	0.0687 (0)	−0.0383 (0)	5.1700 (0)
H(32)	0.0497 (0)	0.6270 (0)	0.1416 (0)	6.0700 (0)	H(62)	−0.1033 (0)	0.1993 (0)	0.0089 (0)	5.1700 (0)
H(33)	0.1217 (0)	0.6299 (0)	0.2318 (0)	6.0700 (0)	H(63)	−0.0647 (0)	0.0504 (0)	0.0058 (0)	5.1700 (0)

[a] The form of the anisotropic thermal parameter is $\exp[-0.25(h^2a^2B(1,1) + k^2b^2B(2,2) + l^2c^2B(3,3) + 2hkabB(1,2) + 2hlacB(1,3) + 2klbcB(2,3))]$ where a, b, and c are reciprocal lattice constants. [b] Estimated standard deviations in the least significant digits are shown in parentheses.

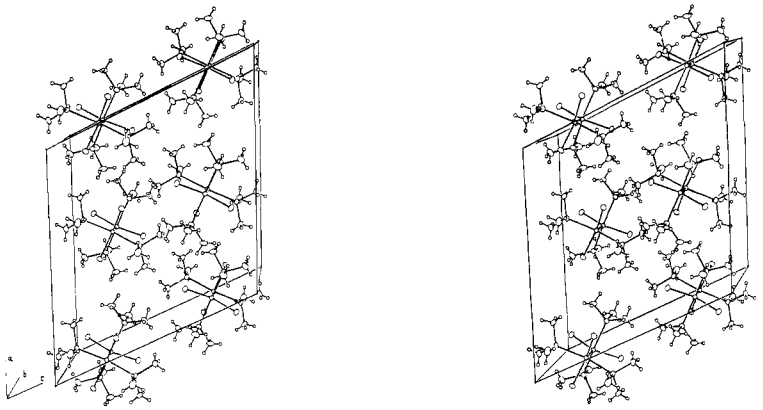

Figure 2. A stereoview of the unit cells of **1a** and **1b** looking down the b axis showing the molecular packing and also showing the essentially eclipsed rotational conformation.

0.04–0.06 Å in **1b**. For the angles esd's were in the range 2–5° for this same compound.

For compound **2** the molecular structure is shown in Figure 3, and the bond lengths and angles are listed in Table VI. A supplementary table (Table VIA) listing bonds and angles involving the hydrogen atoms is again available.

Electronic Absorption Spectra. These were measured by using solutions in dichloromethane and are displayed in Figure 4.

Mass Spectra (Table VII). Both spectra contain peaks assignable to parent ions, M^+, as well as fragment ions produced by sequential loss of chlorine and phosphine ligands. For the molybdenum compound, the main fragmentation pattern consists of sequential loss of PMe_3 ligands from the parent with the $[Mo_2Cl_4(PMe_3)_2]^+$ ion being most abundant. Rupture of the metal–metal bond is not a major process for this species. The tungsten derivative, on the other hand, exhibits a more complex spectrum. Loss of chlorine ligands during fragmentation is competitive with loss of PMe_3. Also, monometallic complex ions are very abundant, indicating that fission of the metal–metal bond is facile under the experimental conditions. In this case, the ion $[MCl(PMe_3)_2]^+$ is the most abundant.

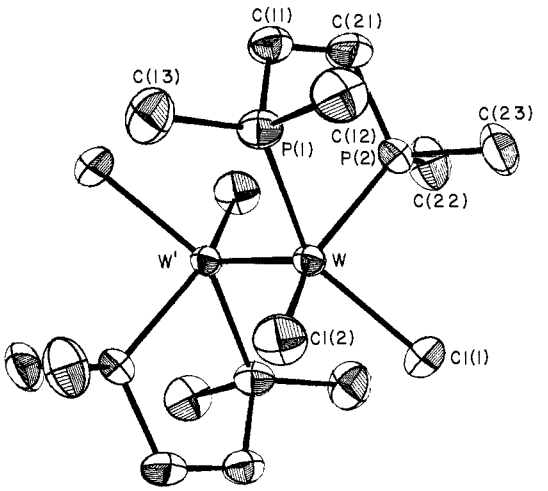

Figure 3. The molecular structure of $W_2Cl_4(dmpe)_2$ (**2**). Atoms are represented by their thermal ellipsoids scaled to enclose 40% of the electron density.

Discussion

Comparison of 1a and 2a. The two $M_2Cl_4(PMe_3)_4$ molecules have qualitatively identical structures but differ in their bond lengths. One difference, that between the Mo—Mo and W—W bond lengths, is fully expected since in all previously available cases of homologous or closely similar molybdenum and tungsten compounds with multiple bonds similar differences, with the W—W bonds being appreciably longer, have existed. However,

Table III. Positional and Thermal Parameters and Their Estimated Standard Deviations for $Mo_2Cl_4(PMe_3)_4$ (1b)[a,b]

atom	x	y	z	B(1,1)	B(2,2)	B(3,3)	B(1,2)	B(1,3)	B(2,3)
Mo(1)	0.0000 (0)	0.33507 (3)	0.2500 (0)	2.031 (8)	2.27 (1)	2.137 (8)	0	0.821 (6)	0
Mo(2)	0.0000 (0)	0.10285 (3)	0.2500 (0)	2.142 (8)	2.27 (1)	1.912 (7)	0	0.753 (6)	0
Cl(1)	−0.10308 (3)	0.43526 (7)	0.12050 (4)	3.42 (2)	3.70 (3)	3.19 (2)	0.56 (2)	0.48 (2)	0.72 (2)
Cl(2)	−0.08580 (3)	0.00400 (7)	0.31053 (3)	3.92 (2)	3.97 (3)	3.78 (2)	−1.00 (2)	2.14 (1)	0.08 (2)
P(1)	0.09602 (3)	0.39385 (7)	0.18334 (4)	3.07 (2)	3.43 (3)	3.65 (2)	−0.08 (2)	1.85 (1)	0.59 (2)
P(2)	−0.11555 (3)	0.04326 (7)	0.10655 (3)	3.01 (2)	3.19 (3)	2.29 (2)	−0.11 (2)	0.54 (2)	−0.32 (2)
C(1)	0.2014 (2)	0.3413 (4)	0.2390 (2)	3.25 (9)	6.8 (2)	7.1 (1)	0.0 (1)	2.74 (7)	2.0 (1)
C(2)	0.0698 (2)	0.3395 (3)	0.0742 (2)	6.5 (1)	5.2 (1)	4.50 (9)	0.1 (1)	3.54 (7)	0.6 (1)
C(3)	0.1011 (2)	0.5912 (3)	0.1778 (2)	6.0 (1)	3.8 (1)	7.1 (1)	−0.7 (1)	3.88 (8)	0.6 (1)
C(4)	−0.1232 (2)	−0.1544 (3)	0.0991 (2)	7.1 (2)	3.6 (1)	5.2 (1)	−0.7 (1)	0.9 (1)	−1.1 (1)
C(5)	−0.2164 (1)	0.0966 (3)	0.0889 (2)	2.82 (9)	5.9 (2)	3.52 (9)	−0.5 (1)	0.48 (7)	−0.1 (1)
C(6)	−0.1099 (2)	0.0958 (4)	0.0083 (1)	5.0 (1)	6.4 (2)	2.61 (8)	0.3 (1)	1.51 (7)	−0.4 (1)

atom	x	y	z	B, Å²	atom	x	y	z	B, Å²
H(11)	0.227 (2)	0.382 (4)	0.207 (2)	7.6 (9)	H(41)	−0.163 (2)	−0.170 (4)	0.048 (2)	7.3 (9)
H(12)	0.203 (2)	0.235 (3)	0.231 (2)	6.5 (9)	H(42)	−0.080 (2)	−0.198 (3)	0.096 (2)	7.9 (10)
H(13)	0.219 (2)	0.376 (4)	0.292 (2)	8.5 (9)	H(43)	−0.125 (2)	−0.206 (4)	0.142 (2)	8.1 (10)
H(21)	0.106 (2)	0.386 (3)	0.058 (2)	6.3 (8)	H(51)	−0.251 (1)	0.057 (3)	0.038 (2)	4.7 (6)
H(22)	0.077 (2)	0.239 (4)	0.071 (2)	7.9 (10)	H(52)	−0.223 (2)	0.206 (3)	0.080 (2)	6.1 (8)
H(23)	0.024 (2)	0.359 (3)	0.045 (2)	5.0 (6)	H(53)	−0.228 (1)	0.071 (3)	0.131 (1)	5.0 (6)
H(31)	0.136 (2)	0.621 (3)	0.153 (2)	5.9 (7)	H(61)	−0.118 (2)	0.199 (3)	−0.001 (2)	6.7 (9)
H(32)	0.052 (2)	0.640 (3)	0.152 (2)	5.7 (7)	H(62)	−0.151 (1)	0.054 (3)	−0.036 (2)	5.9 (7)
H(33)	0.116 (2)	0.631 (4)	0.231 (2)	7.3 (9)	H(63)	−0.066 (2)	0.064 (4)	0.006 (2)	6.9 (8)

[a] The form of the anisotropic thermal parameter is $\exp[-0.25(h^2a^2B(1,1) + k^2b^2B(2,2) + l^2c^2B(3,3) + 2hkabB(1,2) + 2hlacB(1,3) + 2klbcB(2,3))]$ where a, b, and c are reciprocal lattice constants. [b] Estimated standard deviations in the least significant digits are shown in parentheses.

Table IV. Positional and Thermal Parameters and Their Estimated Standard Deviations for $W_2Cl_4(dmpe)_2 \cdot C_7H_8$ (2)[a,b]

atom	x	y	z	B(1,1)	B(2,2)	B(3,3)	B(1,2)	B(1,3)	B(2,3)
W	0.04897 (3)	0.08511 (2)	0.48948 (2)	2.396 (9)	2.15 (1)	1.978 (9)	−0.083 (9)	0.306 (8)	0.041 (9)
Cl(1)	−0.0045 (2)	0.2359 (2)	0.5888 (1)	5.71 (9)	3.10 (7)	3.69 (7)	0.11 (7)	1.18 (7)	−0.83 (6)
Cl(2)	0.3138 (2)	0.1135 (2)	0.5745 (2)	3.00 (0)	4.90 (9)	4.9 (1)	−0.84 (7)	−0.30 (7)	−0.37 (8)
P(1)	0.1282 (2)	0.0308 (2)	0.3455 (1)	2.86 (7)	3.77 (8)	2.90 (6)	−0.18 (6)	1.06 (5)	−0.12 (7)
P(2)	−0.1654 (2)	0.1496 (2)	0.3559 (1)	3.12 (7)	3.08 (7)	2.65 (7)	0.55 (6)	0.26 (6)	0.43 (6)
C(4)	0.0958 (24)	0.0867 (8)	0.0248 (9)	28 (1)	3.7 (5)	5.7 (4)	−0.7 (6)	8.0 (5)	−0.1 (4)
C(5)	−0.0458 (18)	0.1099 (11)	0.0045 (7)	21 (1)	6.8 (6)	4.2 (4)	2.6 (7)	5.9 (5)	0.6 (4)
C(6)	−0.1500 (14)	0.0176 (11)	−0.0219 (8)	10.6 (7)	11.1 (9)	3.9 (4)	−0.7 (7)	2.4 (4)	1.2 (5)
C(7)	−0.2891 (29)	0.0388 (28)	−0.0460 (19)	8 (1)	15 (2)	6 (1)	−2 (1)	2 (1)	2 (1)
C(11)	−0.0387 (8)	−0.0000 (6)	0.2456 (5)	4.2 (3)	4.3 (4)	2.6 (3)	−0.3 (3)	0.8 (2)	−0.4 (3)
C(12)	0.2122 (10)	0.1509 (7)	0.3001 (6)	5.6 (4)	4.8 (4)	5.2 (4)	−1.4 (3)	2.5 (3)	0.4 (3)
C(13)	0.2687 (10)	−0.0748 (8)	0.3451 (7)	4.2 (3)	5.9 (5)	6.1 (4)	1.4 (3)	2.4 (3)	0.2 (4)
C(21)	−0.1688 (10)	0.0777 (7)	0.2402 (6)	4.9 (4)	5.0 (4)	3.1 (3)	1.5 (3)	−0.4 (3)	−0.2 (3)
C(22)	−0.3616 (10)	0.1564 (8)	0.3597 (7)	3.7 (3)	5.6 (4)	5.9 (5)	0.9 (3)	0.6 (3)	0.3 (4)
C(23)	−0.1315 (12)	0.2947 (7)	0.3336 (7)	7.0 (5)	3.9 (4)	4.9 (4)	0.3 (4)	0.7 (4)	1.2 (3)

atom	x	y	z	atom	x	y	z
H(141)*	0.167 (0)	0.146 (0)	0.043 (0)	H(131)	0.379 (11)	−0.069 (7)	0.375 (7)
H(151)*	−0.081 (0)	0.184 (0)	0.007 (0)	H(132)	0.236 (9)	−0.166 (8)	0.355 (6)
H(161)*	−0.256 (0)	0.030 (0)	−0.037 (0)	H(133)	0.290 (11)	−0.085 (7)	0.269 (7)
H(171)*	−0.345 (0)	−0.028 (0)	−0.061 (0)	H(211)	−0.290 (11)	0.070 (8)	0.222 (7)
H(172)*	−0.315 (0)	0.075 (0)	0.007 (0)	H(212)	−0.175 (10)	0.126 (7)	0.201 (7)
H(173)*	−0.313 (0)	0.086 (0)	−0.101 (0)	H(221)	−0.424 (11)	0.086 (7)	0.331 (7)
H(111)	−0.033 (9)	−0.013 (7)	0.181 (7)	H(222)	−0.442 (9)	0.177 (8)	0.275 (6)
H(112)	−0.062 (11)	−0.086 (6)	0.274 (7)	H(223)	−0.372 (10)	0.191 (8)	0.409 (7)
H(121)	0.240 (10)	0.131 (7)	0.253 (6)	H(231)	−0.007 (10)	0.313 (8)	0.340 (6)
H(122)	0.297 (10)	0.176 (8)	0.352 (6)	H(232)	−0.159 (10)	0.309 (8)	0.279 (7)
H(123)	0.161 (10)	0.209 (7)	0.278 (7)	H(233)	−0.132 (10)	0.336 (8)	0.382 (7)

[a] The form of the anisotropic thermal parameter is $\exp[-1/4(B(1,1)h^2a^{*2} + B(2,2)k^2b^{*2} + B(3,3)l^2c^{*2} + 2B(1,2)hka^*b^* + 2B(1,3)hla^*c^* + 2B(2,3)klb^*c^*)]$. [b] Calculated hydrogen atom positions have an asterisk following the atom name. All hydrogen atoms were assigned B_{iso} values of 7.0 Å².

the present difference, 0.132 (2) Å, is the largest such difference so far observed.

Among all triple Mo≡Mo and W≡W bonds the differences are all equal to or less than 0.09 Å. In the $M_2(mhp)_4$,[8] $M_2(map)_4$,[9] and $M_2(dmhp)_4$[10] molecules the differences are 0.096 (2), 0.094 (2), and 0.091 (2) Å, respectively. For the $M_2(C_8H_8)_3$ molecules[11] the difference is 0.073 (2) Å. The largest such difference previously observed is in the $[M_2(CH_3)_8]^{4-}$ ions,[12] where it is 0.116 (2) Å.

The correlation that tentatively emerges from the available data is that when bridging ligands are present, they exert a buttressing effect (whether mainly mechanical or appreciably electronic in

(8) Cotton, F. A.; Fanwick, P. E.; Niswander, R. H.; Sekutowski, J. C. *J. Am. Chem. Soc.* **1978**, *100*, 4725.
(9) Cotton, F. A.; Niswander, R. H.; Sekutowski, J. C. *Inorg. Chem.* **1978**, *17*, 3541.
(10) Cotton, F. A.; Niswander, R. H.; Sekutowski, J. C. *Inorg. Chem.* **1979**, *18*, 1152.
(11) Cotton, F. A.; Koch, S. A.; Schultz, A. J.; Williams, J. M. *Inorg. Chem.* **1978**, *17*, 2093.
(12) Collins, D. M.; Cotton, F. A.; Koch, S. A.; Millar, M.; Murillo, C. A. *Inorg. Chem.* **1978**, *17*, 2017.

Table V. Bond Distances (Å) and Angles (Deg) for the $M_2Cl_4(PMe_3)_4$ Molecules

	M = Mo	M = W
	Distances	
M(1)-M(2)	2.130 (0)	2.262 (1)
M(1)-Cl(1)	2.415 (1)	2.395 (2)
M(1)-P(1)	2.546 (1)	2.509 (2)
M(2)-Cl(2)	2.413 (1)	2.389 (2)
M(2)-P(2)	2.544 (1)	2.506 (2)
P(1)-C(1)	1.820 (4)	1.823 (9)
P(1)-C(2)	1.811 (4)	1.809 (9)
P(1)-C(3)	1.817 (4)	1.797 (9)
P(2)-C(4)	1.819 (4)	1.812 (11)
P(2)-C(5)	1.811 (3)	1.798 (8)
P(2)-C(6)	1.814 (3)	1.812 (8)
	Angles	
M(2)-M(1)-Cl(1)	112.37 (2)	111.74 (6)
M(2)-M(1)-P(1)	102.23 (2)	101.18 (5)
Cl(1)-M(1)-Cl(1')	135.27 (4)	136.9 (1)
Cl(1)-M(1)-P(1)	85.27 (2)	85.88 (7)
Cl(1)-M(1)-P(1')	85.48 (2)	85.88 (7)
P(1)-M(1)-P(1')	155.55 (4)	157.7 (1)
M(1)-M(2)-Cl(2)	112.07 (2)	111.55 (6)
M(1)-M(2)-P(2)	102.41 (2)	101.10 (5)
Cl(2)-M(2)-Cl(2')	135.85 (4)	136.9 (1)
Cl(2)-M(2)-P(2)	85.24 (2)	85.83 (6)
Cl(2)-M(2)-P(2')	85.49 (2)	86.06 (7)
P(2)-M(2)-P(2')	155.18 (4)	157.8 (1)
M(1)-P(1)-C(1)	119.3 (2)	119.0 (3)
M(1)-P(1)-C(2)	119.3 (2)	119.5 (3)
M(1)-P(1)-C(3)	107.3 (1)	107.9 (3)
C(1)-P(1)-C(2)	103.2 (3)	103.0 (5)
C(1)-P(1)-C(3)	103.0 (2)	103.0 (5)
C(2)-P(1)-C(3)	102.4 (2)	102.2 (5)
M(2)-P(2)-C(4)	106.9 (2)	108.4 (4)
M(2)-P(2)-C(5)	118.2 (1)	118.6 (3)
M(2)-P(2)-C(6)	120.1 (1)	120.5 (3)
C(4)-P(2)-C(5)	102.4 (2)	101.0 (5)
C(4)-P(2)-C(6)	103.4 (3)	102.1 (5)
C(5)-P(2)-C(6)	103.6 (2)	103.4 (4)

Table VI. Bond Distances (Å) and Angles (Deg) for $W_2Cl_4(dmpe)_2 \cdot C_7H_8$ (2)

	Distances		
W-W'	2.287 (1)	P(2)-C(21)	1.854 (9)
W-Cl(1)	2.431 (2)	P(2)-C(22)	1.813 (10)
W-Cl(2)	2.418 (2)	P(2)-C(23)	1.816 (11)
W-P(1)	2.444 (2)	C(4)-C(5)	1.28 (3)
W-P(2)	2.455 (2)	C(4)-C(6')	1.35 (2)
P(1)-C(11)	1.818 (8)	C(5)-C(6)	1.44 (2)
P(1)-C(12)	1.835 (10)	C(6)-C(7)	1.25 (3)
P(1)-C(13)	1.809 (9)	C(11)-C(21)	1.499 (12)
	Angles		
W'-W-Cl(1)	116.33 (5)	C(11)-P(1)-C(13)	107.5 (5)
W'-W-Cl(2)	115.82 (5)	C(12)-P(1)-C(13)	100.7 (5)
W'-W-P(1)	95.02 (5)	W-P(2)-C(21)	110.9 (3)
W'-W-P(2)	97.24 (5)	W-P(2)-C(22)	125.3 (4)
Cl(1)-W-Cl(2)	86.38 (8)	W-P(2)-C(23)	107.5 (4)
Cl(1)-W-P(1)	147.22 (7)	C(21)-P(2)-C(22)	105.8 (5)
Cl(1)-W-P(2)	88.28 (6)	C(21)-P(2)-C(23)	104.8 (5)
Cl(2)-W-P(1)	88.36 (7)	C(22)-P(2)-C(23)	100.3 (6)
Cl(2)-W-P(2)	145.27 (8)	C(5)-C(4)-C(6')	124 (2)
P(1)-W-P(2)	77.95 (7)	C(4)-C(5)-C(6)	117 (2)
W-P(1)-C(11)	109.4 (3)	C(5)-C(6)-C(4')	120 (2)
W-P(1)-C(12)	109.6 (4)	C(5)-C(6)-C(7)	118 (2)
W-P(1)-C(13)	124.3 (3)	C(4')-C(6)-C(7)	122 (3)
C(11)-P(1)-C(12)	103.2 (4)		

nature is uncertain) that keeps the W—W quadruple bond length within about 0.09–0.10 Å of the Mo—Mo quadruple bond length. When bridging groups are not present but we are dealing only with the σ and π elements, i.e., with triple bonds, the difference again is less than 0.10 Å. However, when we are dealing with the δ component as well and there are no bridging groups, the W—W bond tends to be 0.11–0.13 Å longer than the Mo—Mo bond. Therefore, we might expect that for the $[W_2Cl_8]^{4-}$ ion, which has not yet been obtained but presumably can be, the W—W distance would be in the range 2.25–2.28 Å, based on the range of 2.14–2.15 Å for the $[Mo_2Cl_8]^{4-}$ ion.[13] Thus, the distance of 2.20 Å used in an SCF Xα–SW calculation[14] on $[W_2Cl_8]^{4-}$, which led to the conclusion that "there does not appear to be any qualitative reason that the $[W_2Cl_8]^{4-}$ ion should not be capable of existence", was carried out a slightly too short W—W distance. However, the discrepancy of 0.05–0.08 Å is so small that the conclusion should not be vitiated. In any event, the present estimate is still only an estimate and could be in error. In the case of $[Tc_2Cl_8]^{2-}$ and $[Re_2Cl_8]^{2-}$ the increase is only about 0.094 Å,[15] which if applicable to the $[Mo_2Cl_8]^{4-}/[W_2Cl_8]^{4-}$ pair puts the W—W distance in the range 2.18–2.19 Å. It is clear that the actual isolation and structural characterization of the $[W_2Cl_8]^{4-}$ ion remains a highly interesting project and that only then will the present uncertainties be resolved.

The other point that arises in comparing the structures of **1a** and **1b** concerns the different lengths of corresponding Mo—L and W—L bonds. It might be expected that, because of the combined effects of the higher atomic number of the tungsten atom and the lanthanide contraction, a given W—L bond length, l_W, and the corresponding Mo—L bond length, l_{Mo}, would stand in the relation $l_W \geq l_{Mo}$. In fact, the reverse is observed in **1a** and

Table VII. Mass Spectral Data for $M_2Cl_4L_4$ (M = Mo, W; L = PMe_3)

M = W			M = Mo	
rel abund[b]	m/z	assignt[a]	m/z	rel abund[b]
23	812	$M_2Cl_4L_4^+$	640	20
57	736	$M_2Cl_4L_3^+$	564	65
9	701	$M_2Cl_3L_3^+$	529	0
57	660	$M_2Cl_4L_2^+$	488	100
17	625	$M_2Cl_3L_2^+$	453	5
49	584	$M_2Cl_4L^+$	412	31
42	548	$M_2Cl_3L^+$	377	15
6	520	$M_2L_2^+$	348	0
2	513	$M_2Cl_2L^+$	342	0
44	478	M_2ClL^+	307	0
29	444	M_2L^+	272	0
95	403	M_2Cl^+	231	0
0	406	$MCl_2L_2^+$	320	7
100	371	$MClL_2^+$	285	0
25	336	ML_2^+	250	0
15	330	MCl_2L^+	244	18
30	295	$MClL^+$	209	14
95	289	MCl_3^+	203	0
39	254	MCl_2^+	168	0
14	184	M^+	98	0

[a] Assignments are made on the basis of the most abundant naturally occurring isotope, i.e., ^{35}Cl, ^{98}Mo, ^{184}W. [b] Peaks due to PMe_3 fragmentation were observed but not included.

Table VIII. Metal-Ligand Bond Lengths in Homologous Molybdenum and Tungsten Compounds

compd	X	l_{Mo-X}, Å	l_{W-X}, Å	Δ,[a] Å	ref
$M_2(mhp)_4$	N(ring)	2.17 (1)	2.12 (2)	0.05 (2)	8
	O	2.086 (6)	2.037 (5)	0.05 (1)	
$M_2(map)_4$	N(ring)	2.18 (1)	2.16 (1)	0.02 (1)	9
	N(exo)	2.14 (1)	2.10 (1)	0.04 (1)	
$M_2(dmhp)_4$	N(ring)	2.157 (4)	2.14 (2)	0.02 (2)	10
	O	2.077 (4)	2.056 (6)	0.012 (7)	
$[M_2(CH_3)_8]^{4-}$	C	2.29 (1)	2.32 (2)	−0.03 (2)	12
$M_2Cl_4(PMe_3)_4$	Cl	2.414 (1)	2.392 (2)	0.022 (2)	this work
	P	2.545 (1)	2.507 (2)	0.038 (2)	

[a] $\Delta = l_{Mo-X} - l_{W-X}$.

(13) Brencic, J. V.; Cotton, F. A. *Inorg. Chem.* **1970**, *9*, 346.
(14) Cotton, F. A.; Kalbacher, B. J. *Inorg. Chem.* **1977**, *16*, 2386.
(15) Cotton, F. A.; Daniels, L.; Davision, A.; Orvig, C., unpublished work.

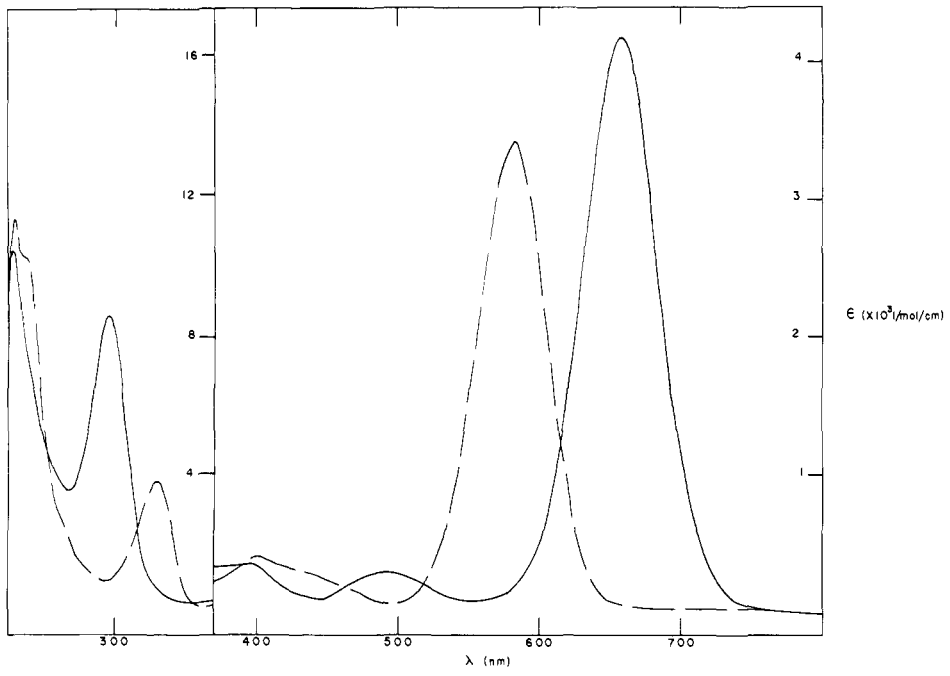

Figure 4. The visible and near-ultraviolet spectra of $MoCl_4(PMe_3)_4$ (---) and $W_2Cl_4(PMe_3)_4$ (—) measured in dichloromethane solution.

1b. For the M—Cl distances we have $l_{Mo} - l_W = 0.022$ (2) Å and for the M—P distances the corresponding differences are 0.038 (2) Å.

This is not an entirely new result though previous examples of it have been less distinct because of greater uncertainties in individual observed bond lengths and/or the existence of appreciable variation among crystallographically distinct bonds of the same type chemically. The data for the $M_2(mhp)_4$,[8] $M_2(map)_4$,[9] and $M_2(dmhp)_4$[10] cases are summarized in Table VIII. Although the differences are less significant than those in the $M_2Cl_4(PMe_3)_4$ molecules because of the larger uncertainities, they are of the same magnitude and sign; i.e., $l_{Mo} > l_W$. For the $[M_2(CH_3)_8]^{4-}$ ions the reverse trend, $l_W - l_{Mo} \approx 0.03$ Å, is found, but the confidence level here is particularly low.

Compounds **1a** and **1b** also afford an interesting comparison with respect to their electronic absorption spectra, shown in Figure 4. Only the $\delta \rightarrow \delta^*$ bonds in the 500–700-nm region will be discussed here. Because of the greater W—W distance a smaller δ–δ overlap would be expected. This, in turn, would lead us to expect[16] (a) that the $\delta \rightarrow \delta^*$ transition should occur at lower energy and (b) that it might be of lower intensity in $W_2Cl_4(PMe_3)_4$ than in $Mo_2Cl_4(PMe_3)_4$. The first expectation is fulfilled, with the band being at 17.19×10^3 and 15.21×10^3 cm^{-1} for the molybdenum and tungsten compounds, respectively. However, the intensity of the band in the tungsten compound is about 20% greater. The relationship between intensity and bond overlap is only a semiquantitative one and cannot be expected always to give correct predictions when the differences are small, as in the present case. The shift in position of the bands from the molybdenum to the tungsten compound is similar to that previously observed[17] in the $[M_2(CH_3)_8]^{4-}$ ions. Because of the extreme sensitivity of the $[M_2(CH_3)_8]^{4-}$ ions to air and moisture, these species do not afford a reliable source of information on relative intensities.

The mass spectra fragmentation patterns of **1a** and **1b** present an interesting and significant contrast. The majority of the fragments from $Mo_2Cl_4(PMe_3)_4$, including the major one, are binuclear whereas for $W_2Cl_2(PMe_3)_4$ the major ion and a large number of others are mononuclear. While the relationship of this kind of data to thermodynamically meaningful bond strength estimates is uncertain, the clear implication seems to be that the W≡W bond is not as strong as the Mo≡Mo bond.

The Structure of 2. The structure of $W_2Cl_4(dmpe)_2$ is of unusual interest because it is one of the first two examples, the other being the green isomer of $W_2Cl_4(dppe)_2$, of a quadruply bonded dimetal complex in which diphosphine ligands are chelated instead of bridging. It, therefore, also provides one of the first two examples of an $M_2X_4(Phos)_4$-type molecule in which the $MX_2(Phos)_2$ unit has a cis instead of a trans arrangement. This results in the W—W bond being significantly longer, 2.287 (1) Å, than that in **1a**, 2.262 (1) Å. We see no simple explanation for this.

There are also differences in the W—Cl and W—P bond lengths in **1a** and **2**, and these seem to be manifestations of structural trans influences similar to those found in the square complexes of the platinum group metals. Thus, for **1a**, where we have W—P trans to W—P, and in **2** where W—P is trans to W—Cl, the W—P bond lengths are 2.508 (2) and 2.450 (5) Å, with the highly significant difference of 0.058 (5) Å indicating a trans weakening effect by PR_3 relative to Cl. Similarly for the W—Cl bonds trans to W—P (in **2**) and trans to W—Cl (in **1a**), the bond lengths are 2.426 (7) and 2.392 (3) Å, with a difference of 0.034 (8) Å, which is also statistically significant. These evidences of trans influence in quadruply bonded compounds will be examined in more detail in a subsequent paper dealing with the structures of the isomeric $W_2Cl_4(dppe)_2$ molecules.

Acknowledgment. We thank Professor Richard R. Schrock of MIT for gifts of the tungsten compounds. B.W.S.K. is the recipient of a NATO postdoctoral fellowship from the Natural Science and Engineering Research Council of Canada. This work was supported by the National Science Foundation.

Supplementary Material Available: Tables of observed and calculated structure factors and bonds and angles involving hydrogen atoms for compounds **1a**, **1b**, and **2** (28 pages). Ordering information is given on any current masthead page.

(16) Cotton, F. A. *Pure Appl. Chem.* **1980**, *52*, 2331. The relative intensities of the bands shown in Figure 1 in this paper are in error; they were based on preliminary measurements and the spectra now reported supercede those in this reference.

(17) Sattelberger, A. P.; Fackler, J. P.; Jr. *J. Am. Chem. Soc.* **1977**, *99*, 1258.